

Removal of Order Domain Content in Rotating Equipment Signals by Double Resampling

By:

Charles L. Groover
Martin W. Trethewey

Department of Mechanical and Nuclear Engineering
Penn State University
University Park, PA 16802
USA

Kenneth P. Maynard
Mitchell S. Lebold
Applied Research Laboratory
Penn State University
University Park, PA 16802
USA

Submitted to:

Mechanical Systems and Signal Processing

Corresponding Author:

Martin W. Trethewey
329 Reber Building
Penn State University
University Park, PA 16802
USA

Email: mwtrethewey@psu.edu
FAX: + 814-865-9693

Submitted:
June 2003

Revised:
September 2003

Abstract

Fixed frequency content (i.e., component or structural resonances) in spectra obtained from rotating equipment can be masked by the strong sources at harmonics (order) of the shaft running speed. The ratio of the fixed frequency components to the order components can be greater than 60 dB making interpretation of resonances in the spectra difficult. Hence the order components are view as a corrupting phenomenon. An approach to remove the order components from the spectra, without affecting the remaining frequency domain information is presented in this work. The technique utilizes a sequence of data sampling and transformations, between the time, order and frequency domains as follows:

1. Vibration data is sampled using a constant time basis (Δt).
2. The times corresponding to a constant angular basis ($\Delta\theta$) are determined.
3. The vibration data is interpolated to a constant angular basis ($\Delta\theta$).
4. The constant angle sampled data is transformed via the FFT to the order domain.
5. The high amplitude order components are now exactly bin centered and can be removed from the spectra.
6. An inverse FFT is applied to return to a constant angular increment sampled ($\Delta\theta$) array, sans order content.
7. The constant angular increment sampled ($\Delta\theta$) array is interpolated to an array sampled with constant time basis (Δt).
8. A FFT is applied and then standard spectral estimation procedures are applied to compute the vibration spectra with the high level orders removed.

The theoretical and implementation details of the double resampling approach are discussed. The approach is applied to experimental torsional vibration data acquired from a laboratory test rig designed to simulate a turbine rotor. The test results show that the method can recover fixed frequency components (i.e., turbine blade natural frequencies) in the presence of order components 50 dB higher.

1. Introduction

Forced vibration in rotating equipment can generally be separated into two categories; 1) variable frequency components related to the machine's rotation rate; and 2) fixed frequency related vibration. Spectral analysis is commonly used to separate and identify the frequencies of importance. For synchronous machines all the frequency components remain fixed regardless if they are caused by the machine's inherent rotation (e.g., imbalance) or a fixed frequency component (e.g., structural resonance). However, for asynchronous machines the running speed changes, either drifting or experiencing rapid speed changes depending on the application. In this case, all the vibration related to a machine's rotation (i.e., imbalance) change proportionately in frequency to the running speed variations while the fixed frequency components remain constant.

To track the frequency variations in relation to changes in the equipment running speed, order analysis is used. Frequency and order analysis are similar, but with different independent arguments. Frequency analysis applies a Fourier transform to a vibration signal digitized with a uniform sampling time interval (Δt). The resulting spectrum's independent variable is in Hz. Order analysis applies a Fourier transform to a vibration signal sampled on the basis of a uniform angular shaft rotation increment ($\Delta\theta$). The independent spectral variable is orders, or multiples of shaft running speed. Hence, any vibration directly caused by the machine's rotational speed will remain at a fixed order regardless of running speed. A significant body of work exists both in order processing algorithms [1,2,3] and applications [4,5].

Order analysis has proven to be effective to track vibration components in relation to variation in running speeds. However, an artifact of the transformation from the

frequency domain to the order domain is that all fixed frequency components (i.e., resonance vibration) will change orders as the running speed varies. Therefore, in applications where fixed frequency components are important, frequency based analysis is appropriate. Whereas, when rotational related components are important, order analysis is appropriate. In some applications both are important and it is necessary to be able to separate the components.

A very demanding application requiring accurate frequency identification in the presence of rotational dependent components is found in the health monitoring of turbine blades [6] in turbomachinery. The monitoring method uses the turbine blade “bending” natural frequencies as a structural health diagnostic feature. The blade natural frequencies are detected by analysis of the rotating shaft torsional vibration signature. As a crack develops in a blade its natural frequency drops. Hence, the measurement of the blade frequencies can be ultimately used as a diagnostic metric to monitor the structural integrity of the blade. The detection of the blade frequencies in the torsional domain requires that blade modes couple with shaft torsional modes. Because of the physical scale of the blades to the shafting, the blade bending to shaft torsion coupling produces very small torsional vibration levels. The relatively large amplitude vibration caused by rotational related components further compounds the detection of the blade frequencies. The high level rotation components can potentially make the harvesting the very small signals associated with blade vibration in the torsional domain very difficult, if not infeasible.

Other examples of problems of this type may be found when it is necessary to separate fixed order from fixed frequency components. For example, gear tooth health

diagnostics in drive trains and gearboxes [7]. Again, the bending frequencies of the gear teeth are monitored and used as a health diagnostic feature and can difficult to distinguish from the strong order components.

Impact testing can be used to identify the natural frequencies in rotating equipment while operating [8]. When the vibration response is acquired from an impact, it will inherently include the fixed frequency resonances and the rotating related components. The fixed order components need to be identified and separated to enable identification of the natural frequencies. The ratio of the fixed frequency components to the order components can be greater than as 60 dB making interpretation of resonances in the spectra difficult. Hence, the order components are viewed as a corrupting phenomenon.

An approach to remove the order components from the spectra, without affecting the remaining frequency domain information is presented in this work. The technique utilizes a sequence of data sampling and transformations, between the time, order and frequency domains as follows:

1. Vibration data is sampled using a constant time basis (Δt).
2. The times corresponding to a constant angular basis ($\Delta\theta$) are determined.
3. The signal amplitudes corresponding to the constant angular basis ($\Delta\theta$) are determined via a computed order resampling interpolation.
4. The constant angle sampled data block is transformed via the FFT to the order domain.
5. The high amplitude order components are now exactly bin centered and can be removed from the spectra, without affecting data in adjacent bins.

6. The order domain spectral data block, sans order content, is inverse transformed back to an array sampled with a constant angular basis ($\Delta\theta$).
7. The constant angle interval array is interpolated back to a contact time interval array (Δt).
8. An FFT and standard spectral estimation procedures are then applied to estimate the frequency based vibration spectra with the high level orders removed.

In the following sections the theoretical basis of the order removal method will first be presented. The processing technique will then be demonstrated with torsional vibration data acquired from a laboratory test stand. The paper concludes with an assessment of the method's capabilities.

2. Double Resampling for Order Content Removal

Consider a simulated analog data signal and the synchronous keyphasor signal from a hypothetical piece of rotating equipment. The simulated signal could represent a number of possible physical measurements including, an accelerometer, microphone, load cell, strain gage, etc. and will use generic units of voltage in this discussion. The signal and keyphasor are shown in Fig. (1). Fig. (1A) shows a fixed frequency 20 Hz signal superimposed on a higher amplitude signal which is increasing in frequency. The keyphasor signal, Fig. (1B), shows a sharp pulse occurring once every shaft revolution. It is obvious from the keyphasor that the shaft speed is accelerating since the time between the keyphasor pulses is decreasing. The frequency spectrum of the signal is shown in Fig. (2). The 20 Hz fixed frequency component is clearly identifiable along with broader low frequency content around 2-3 Hz associate with the changing shaft speed. As the shaft

speed increases the fixed rotation component would eventually dominate the 20 Hz fixed frequency component when the frequencies coincide. It is this possible corrupting facet of the rotational related components that arise in some applications and is the motivation for this effort.

To simplify the identification of low level fixed frequency spectral features in the presence of high level shaft speed harmonics is presented in this section. The method utilizes a series of resampling interpolations along with forward and inverse Fourier transforms as follows:

Step 1: Fixed Time Sample Data Acquisition – First, a sufficiently long discrete data array from an analog transducer signal, $x(t)$, on the rotating equipment operating at the desired conditions is acquired.

$$x(t_r) = x(r \Delta t) \quad (1)$$

where r is an integer index and Δt is the time based sampling interval. The sample rate should be appropriate for the desired analysis frequency range and anti-alias protected by the use of filters.

A once per revolution key phasor signal synchronized to the acquired dynamic signal should also be recorded. The key-phasor tachometer signal should use a significantly higher sample rate as to provide a very accurate estimate of the shaft speed.

Fig. (3) depicts the analog signal with the discrete array superimposed when digitized with a fixed sampling frequency. Note, that there are varying numbers of discretized data points during each respective cycle of the shaft's rotation. This is directly due to using a fixed frequency sampling rate applied to an angularly accelerating shaft.

Step 2: Fixed Angular Sample Time Identification – A computed order tracking algorithm is now utilized to change the independent variable to the shaft rotation angle (θ) from time (t). The discrete angular sampling process will produce a discrete array with an identical number of discretized data points per shaft revolution, regardless of the speed. The angular based sampling interval is defined as:

$$\Delta\theta = \frac{360^\circ}{O} \quad (2)$$

where O represents an integer number of angular increments around the shaft. The angular discretization produces the array:

$$x(\theta_r) = x(r\Delta\theta) \quad (3)$$

where r is an index.

The computed order interpolation method to obtain the array in Eqn. (3) was first proposed in [1] and has proven to be effective and robust. The first step is the determination of the times that correspond to the fixed angular sampling intervals, ($r\Delta\theta$). Calculation of these new sampling times requires an accurate reference of the shaft rotation. Accuracy of the fixed angle sampling times is highly dependent upon correctly detecting the edge of the tachometer signal. After acquiring accurate keyphasor times, the desired times corresponding to $r\Delta\theta$ can be determined. The assumption that the reference shaft experiences a constant acceleration is made [1] in order to create the relationship between shaft angular position and time:

$$\theta(t) = b_0 + b_1t + b_2t^2 \quad (4)$$

The coefficients of Eqn. (4) can be determined by solving three independent equations using the times (t_1, t_2, t_3) recorded for three contiguous keyphasor pulses, as shown in Eqn. (5).

$$\begin{bmatrix} 0 \\ 1 \\ 2 \end{bmatrix} = \begin{bmatrix} 1 & t_1 & t_1^2 \\ 1 & t_2 & t_2^2 \\ 1 & t_3 & t_3^2 \end{bmatrix} \begin{bmatrix} b_0 \\ b_1 \\ b_2 \end{bmatrix} \quad (5)$$

The solution of Eqn. (5) for the coefficients yields [1]:

$$b_0 = \frac{t_1 [t_3(t_1 - t_3) + 2t_2(t_2 - t_1)]}{(t_2 - t_1)(t_3 - t_1)(t_3 - t_2)} \quad (6)$$

$$b_1 = \frac{t_1^2 + t_3^2 - 2t_2^2}{(t_2 - t_1)(t_3 - t_1)(t_3 - t_2)} \quad (7)$$

$$b_2 = \frac{2t_2 - t_1 - t_3}{(t_2 - t_1)(t_3 - t_1)(t_3 - t_2)} \quad (8)$$

Once the coefficients have been determined, the desired sampling times can be calculated by solving quadratic Eqn. (4) for time as a function of angular shaft position ($r\Delta\theta$). Two solutions exist, but only one yields realistic results (positive values of time) as shown in Eqn. (9):

$$t(\theta_r) = \frac{\sqrt{b_1^2 + 4b_2(\theta_r - b_0)} - b_1}{2b_2} \quad (9)$$

where: r is an integer and $\theta_r = r\Delta\theta$.

New polynomial coefficients from Eqns. (6), (7) and (8) are determined for every new keyphasor pulse. The desired sampling times are calculated over the range of $0.5 \leq \theta_r \leq 1.5$ for each polynomial in order to avoid the overlap between the consecutive

coefficient solutions. The only requirement is that the record be both an integer number of shaft revolutions and an integer multiple of $\Delta\theta$ [1].

The approximation used to create Eqn. (4) enables this method to correctly track a system with constant acceleration. More complex models of the shaft rotation are possible, but the increased computation time involved and lack of increased accuracy have not warranted their application. Errors due to a physical system not fully satisfying the approximation are generally small, since the coefficients are updated for each tachometer pulse.

Step 3: Computed Fixed Angular Interval Sample Interpolation – Now that the times corresponding to the fixed angular interval sample have been calculated ($t(\theta_r)$), the signal amplitude values at these respective times must be determined. The discrete amplitudes of original rotating equipment signal, $x(t)$, are known only at values corresponding to t_r . Since the times $t(\theta_r)$ will in general be different, an interpolation is necessary. Various interpolation schemes may be used to obtain the fixed angle sampled signal amplitudes, $x(\theta_r)$, from the fixed time sampled data array $x(t_r)$ [9]. The routine used in [1], entails oversampling the signal by expanding the original time vector and applying a finite impulse response (FIR) filter. The FIR filter allows the original data to pass through and interpolates between the values so that the mean squared errors are minimized. The method in [1] uses an oversampling factor of 2 along with a 10-point FIR filter designed to give a passband flatness of $\pm 0.08\%$ and a stopband rejection greater than 104 dB [1]. To improve the computational speed the actual filter used in this algorithm is implemented as a lookup table stored in the memory. This leads to some round off error yielding a dynamic range closer to 80 dB [10].

An alternative interpolation was implemented in this work. After the desired fixed angle sampling times have been determined, $t(\theta_r)$, the next step is to up-sample the data in order to enable the use of a simple interpolation method. The discrete time sampled data array, $x(t_r)$, was increased by an up-sampling factor of 32 producing a well defined waveform. A cubic spline interpolation was used to calculate the signal amplitudes corresponding to the desired constant angle sampling times, $t(\theta_r)$ from the up-sampled array. Cubic spline interpolation was shown to have the least amount of error when used in this type of application [2,11]. The process produced a new constant angle sampled data array $x(\theta_r)$. The actual coding used the Matlab “interp1” command [12].

A graphical depiction of the constant angle interpolation, $x(\theta_r)$, from the fixed time step sampled data, $x(t_r)$, is shown in Fig. (4). The original analog signal is graphed as a solid line and a blown up time segment of the data in Fig. (3) is shown. The constant time sampled data is marked by the asterisk (*) symbol. This data is the discrete array that would be available from the analog-to-digital converter. The diamond (\diamond) marked points represent the discrete waveform amplitude when sampled with respect to a constant angle of rotation ($\Delta\theta$). The time values corresponding to the angular increments are determined by the procedure discussed in step 2 and the interpolation process described herein estimates signal amplitudes.

Step 4: Order Domain Spectral Estimation – A FFT algorithm is now applied to the constant angle sampled data array, $x(\theta_r)$ by;

$$X(o_n) = \sum_{r=0}^{N-1} x(\theta_r) e^{-i\left(\frac{2\pi n r}{N}\right)} \quad (10)$$

The order spectrum in units of (v_{rms}^2) can be calculated from Eqn. (10) and is shown in Fig. (5). It clearly shows the high amplitude component related to the first order, or the shaft rotational running speed. Unlike the frequency based spectrum in Fig. (2), this component does not smear as the running speed changes. Whereas the fixed frequency component at 20 Hz in Fig. (2) becomes smeared as the shaft rotational speed increases.

Step 5: Order Removal – The corrupting high magnitude order content can now be removed from the signal. The key to the removal is the fact that all the order components are exactly bin centered due to angular based sampling, as seen in Fig. (5). The index k that corresponds to integer orders in the spectrum computed from the FFT in Eqn. (10) can be determined from Eqn. (2), producing Eqn (11).

$$k = j(\Delta\theta O) \quad (11)$$

where j is an integer and $1 \leq j \leq \frac{N}{\Delta\theta O}$. The upper limit of j can be adjusted to a lower value or to only troublesome orders if desired.

It is at these values in the order spectrum that it is desirable to remove their effects from the signal. Furthermore, it is important to retain fidelity in both the real and imaginary values of the spectrum since an inverse Fourier transform will be applied later. To accomplish the order content removal several alternative methods were evaluated. A direct zeroing of the order content was unrealistic, since it did not compensate for the signal levels from other sources. This was particularly problematic when an order and a resonance were in the same region. An alternative method uses a linear interpolation of the bins' complex values directly surrounding each integer order.

$$\tilde{X}(o_k) = \frac{\text{Re}[X(o_{k-1})] + \text{Re}[X(o_{k+1})]}{2} + i \frac{\text{Im}[X(o_{k-1})] + \text{Im}[X(o_{k+1})]}{2} \quad (12)$$

where the index k is defined in Eqn. (11). Note, the symbol $\tilde{}$ is used to denote a quantity in which the order content has been removed.

The method expressed in Eqn. (12) was found to work reasonably well, but occasionally encountered difficulties. When processing signals from a system that have well-defined phase shifts [13], such as a synchronous motor drive, the removal was ineffective.

An alternative method based on the local complex minima surrounding an integer order is shown in Eqn. (13):

$$\tilde{X}(o_k) = \min[X(o_{k-1}), X(o_{k+1})] \quad (13)$$

This method was found to be more robust with actual experimental data under various operational conditions [13]. Hence, it is used subsequently in this work.

Fig.(6) depicts the order domain spectrum with the first order content removed. It is apparent that the high amplitude first order content is absent while the remaining part of the spectrum is unaffected.

Step 6 – Fixed Angular Interval Array Without Order Content – An inverse FFT is now applied to the order domain array, $\tilde{X}(o_n)$.

$$\tilde{x}(\theta_r) = \sum_{r=0}^{N-1} \tilde{X}(o_n) e^{i\left(\frac{2\pi n r}{N}\right)} \quad (14)$$

This produces a constant angle sampled array in which the integer related order content has been removed.

Step 7 – Interpolation to Fixed Time Sample Array Without Order Content –

A reverse operation to Step 3 is now performed whereby the fixed angular sampled array is interpolated to a fixed time sample array. Recall that the times corresponding to the angular sample basis (θ_r) are equal to $t(\theta_r)$. The signal $\tilde{x}(\theta_r)$ is interpolated to obtain the signal amplitudes that occur on a constant time base sample, t_r . This results in a fixed time sampled array, $\tilde{x}(t_r)$, with the order content removed. Similar to the coding in Step 3, the implementation uses the Matlab “interp1” command with a cubic spline [12].

The results of Steps 6 and 7 when applied to the data shown in Fig. (6) is shown in Fig. (7). The resulting time waveform is a sine wave without the high amplitude order related components seen in the original waveform in Fig. (1).

Step 8 – Frequency Based Spectral Estimation Without Order Content – The FFT algorithm is now applied to the discrete time sampled array, $\tilde{x}(t_r)$, to compute a frequency based transform.

$$\tilde{X}(f_n) = \sum_{r=0}^{N-1} \tilde{x}(t_r) e^{-i\left(\frac{2\pi n r}{N}\right)} \quad (15)$$

Data windows and ensemble averaging methods are applied in conjunction with Eqn. (15) to improve the quality of the spectral estimates. The resulting spectrum is shown in Fig.(8). Comparison to Fig. (2) shows that the order content is effectively removed leaving only the fixed frequency components in the spectrum.

3. Capabilities of Fixed Order Content Removal Procedure

The capabilities of the order removal process will be examined using actual experimental vibration data from a rotating equipment test rig. Consider a commonly

used system to measure torsional vibration of a rotating shafting system [14,15] as shown in Fig (9). Signal detection involves four main aspects; shaft encoding; transduction; analog demodulation; and data discretization. The shaft encoding used a target “zebra” strip with alternating black and white stripes printed on paper or polyester and glued to the shaft. Alternate methods include the use of a timing gear or optical encoder. The transducer was an infrared intensity based reflective fiber optic sensor. An analog demodulator was used to produce a voltage signal proportional to the shaft torsional vibration from the carrier signal generated by passage of zebra tape on the rotating shaft. The voltage from the demodulator is then discretized for further processing, such as spectral analysis. The implementation and utilization of this hardware configuration for torsional vibration measurement was previously presented in [15].

Fig. (10) shows a picture of a laboratory test rig developed to study torsional vibration of a shaft with a simulated bladed disk assembly. The shaft is suspended by oil impregnated flanged brass bearings, and is driven by a 1/7th hp motor, with a maximum speed of 10,000 rpm, using a DC power supply. At the opposite end of shaft from the motor was a simulated bladed disk assembly. Eight stainless steel threaded rods are used to represent the blades. Two lock nuts are positioned at the end of each rod to produce a movable mass. The movable nuts allow changes to be made in each rod’s natural frequencies by changing their respective radial location.

The instrumentation followed the signal detection schematic diagram in Fig (9). The encoding zebra tape consisted of 160 black and white lines mounted onto an aluminum wheel next to the drive motor. A single black stripe on the side of the

aluminum wheel created a one per revolution keyphasor. Two fiber optic probes were positioned to sense the zebra tape and the keyphasor as shown in Fig. (11).

Torsional vibration data was collected while the system rotated at a constant speed of approximately 3400 rpm. The data was acquired with a fixed sampling frequency and processed with an Agilent (HP) E1433B card in a VXI mainframe. The spectrum was calculated via a FFT algorithm using 30 ensemble averages and is shown in Fig. (12). The spectrum shows high amplitude content at integer multiples of the nominal 57 Hz running speed, or at fixed orders. The coupled blade bending-torsional mode occurs around 210 Hz and is barely apparent in the spectrum. The shaft torsional mode is at approximately 260 Hz and is almost unnoticeable. The high amplitude order content obscures the low level torsional natural frequency signals. The “skirts” on the fixed order content is caused by leakage due to the nonperiodic capture of the signal.

The corrupting high amplitude order content results from the zebra tape encoding approach. Ideally the zebra tape has identical sections of alternating black and white stripes. However several pragmatic issues related to printing and installation introduce errors caused by:

1. **Printer resolution.** The printer may be incapable of exactly reproducing the desired zebra strip width due to the dpi (dots-per-inch) resolution. This introduces a bias error whereby strips are produced with varying numbers of printed raster lines.
2. **End effects.** When installing the tape around the shaft circumference there may be an overlap or void when attempting to match the first and last stripe

on the shaft. This produces a distinctly different response than the evenly spaced stripes and occurs at a once per revolution cycle.

3. **Tape installation errors.** In theory the tape stripes should be installed parallel to shaft axis. Practically this is difficult to accomplish. Also, the tape may stretch when placing it around the shaft. These errors produce a systematic pattern for every revolution of the shaft that deviates from the ideal regularly spaced condition.

These errors manifest themselves as spectral content frequencies that are integer multiples of the shaft running speed. The data in Fig. (12) was acquired with the shaft rotating at a constant speed. The corrupting nature of the order component would further exacerbate the identification of the fixed frequency components if the running speed were to vary. As the running speed changes the spectral frequencies would change proportionately. Hence, even broader high amplitude frequency regions would result having the potential to dominate and completely obscure the identification of a natural frequency. This example was selected because it clearly demonstrates the corrupting nature that fixed order related components can have on fixed frequency components. Furthermore, it represents a rather severe set of conditions and hence serves an excellent case to illustrate the proposed method to eliminate the order content from the spectrum.

Data is again collected from the test stand, but this time the processing discussed in Section 2 are applied. The discrete time data array and keyphasor time stamps were acquired by the Agilent VXI system. The data was processed using a routine programmed in Matlab. For the sake of brevity, only critical graphics associated with the performance of the algorithm to the order removal will be presented. Fig. (13) shows one record after

Steps 1-4 have been applied. For visual clarity, a \square symbol marks each bin individually. The high amplitude order content is at exact multiples of the shaft running speed. Furthermore, its bin-centered nature is visible by the fact that only one data point possesses the high amplitude with the adjacent bins being considerably lower amplitude. This character is in contrast to the “skirt” behavior of the frequency spectrum in Fig. (12) and is the key to the ability to remove it. The results after the order removal process is described in Step 5 is applied to the same data sample is shown in Fig. (14). The corrupting order content is now gone. Next, steps 6-8 are then completed. The process is repeated to obtain a total of 30 ensemble frequency records that are averaged together. The final spectrum, with the order content removed, is shown in Fig. (15). Note, that the torsional natural frequencies of the shafting system that were almost non apparent in the original spectrum in Fig. (12) can be readily identified. Furthermore, comparing the results in Fig. (12) to Fig. (15) demonstrates that a dramatic improvement in the effective dynamic range is realized.

4. Concluding Remarks

This work has discussed an algorithm by which order related spectral content can be separated and removed from fixed frequency content on signals acquired on rotating equipment. The processing enhancement is produced by a sequence of digital resampling to facilitate transformation between the time, order and frequency domains. Processing in the respective domains allows the masking effect of the high level order components to be eliminated. The required interpolations and Fourier transforms have been coded in Matlab for evaluation of the method. The algorithm has been shown not only to be

effective in removing the fixed order content but also improves the effective dynamic range by removing the order related “skirts” in the frequency domain.

Laboratory tests clearly demonstrated the proposed method’s ability to improve torsional vibration signals allowing the detection of low amplitude signals. The approach has been applied in several other demanding situations with excellent results. A laboratory test was performed where a fixed frequency torsional mode coincided with an integer multiple of the running speed [13]. Initially the low amplitude fixed frequency component was completely masked by the order component. After application of the order removal algorithm, presently herein, the torsional component was readily identifiable. A field test was also performed on a three-megawatt hydroelectric power unit to demonstrate the potential to apply this data processing algorithms in an industrial environment [13, 15]. This test showed that application of the proposed method produced a more useful torsional vibration signature than the originally acquired data. Furthermore, it demonstrate its ability to handle issues that often arise in the field that may not be apparent in the more controlled laboratory setting.

More investigation is necessary to more fully characterize and quantify the algorithm’s capabilities. The processing relies on a sequence of interpolations, which has potential sources of error. Alternative interpolation schemes should be tried. Because most interpolation methods are based upon polynomials, which require a well-defined signal to be accurate, this method was initially used to facilitate both resampling steps, time-to-order-resampling and order-to-time resampling. If a Fourier series interpolation method could be applied to both steps then the required oversampling could be reduced while still yielding accurate results [16]. This interpolation scheme could, therefore

reduce the computational and memory demands. A thorough error analysis of the various interpolation schemes is needed to evaluate how these inherent errors will manifest themselves in the respective spectra.

Experience with the algorithm to date, has yielded excellent results in several demanding torsional vibration laboratory and field measurement situations. This bodes well for the algorithm's potential in applications where it is desired to separate fixed frequency from order components.

References

1. Potter, R., and Gribler, M. 1989 SAE Paper 891131. Computed Order Tracking Obsoletes Older Methods.
2. Fyfe, K. R., and Munck, E. D. S., 1997 Mechanical Systems and Signal Processing, 11(2). Analysis of Computed Order Tracking.
3. Vold, H. and Leuridan, J., 1993 SAE Paper 931288. High Resolution Order Tracking at Extreme Slew Rates Using Kalman Tracking Filter.
4. Vold, H., Herlufsen, H., Marins M., and Corwin-Renner, D., 1997 Sound and Vibration, 31(5). Multi Axle Order Tracking with Vold-Kalman Tracking Filter.
5. Agilent Technologies, Palo Alto, CA, USA. Effective Machinery Measurements Using Dynamic Signal Analyzers, Application Note AN-243-2.
6. Maynard, K. P., and Trethewey, M. W., 1999 Proceedings of the 53rd Meeting of the Society for Machinery Failure Prevention Technology, Virginia Beach, Virginia, USA April 19-22. On The Feasibility of Blade Crack Detection Through Torsional Vibration Measurements.
7. McFadden, P.D., 1987 Mechanical Systems and Signal Processing 1(2). Examination of a Technique for the Early Detection of Failure in Gears by Signal Processing of the Time Domain Average of the Meshing Vibration.
8. Marscher, W.D., 1999 Proceedings of the 17th International Modal Analysis Conference, Society for Experimental Mechanics. The Determination of Rotor Critical Speeds while Machinery Remains Operating through Use of Impact Testing.
9. IEEE Programs for Digital Signal Processing, 1979 IEEE press, New York, John Wiley & Sons.
10. McDonald, D., and Gribler, M, 1991 Proceedings of the 9th International Modal Analysis Conference, Society for Experimental Mechanics. Digital Resampling: A Viable Alternative for Order Domain Measurements of Rotating Machinery.
11. Munck, E.D.S., 1994 MS Thesis, University of Alberta, Canada. Computed Order Tracking Applied to Vibration Analysis of Rotating Machinery.
12. Matlab, The MathWorks, Inc. Natick, MA, USA.
13. Groover, C.L., 2000 MS Thesis, Department of Mechanical and Nuclear Engineering, Penn State University. Signal Component Removal Applied to the Order Content in Rotating Machinery.
14. Vance, J. M., 1988 Rotordynamics of Turbomachinery, John Wiley & Sons, New York.
15. Maynard, K.P, Trethewey, M.W. and Groover, C. L., 2001 55rd Meeting of the Society for Machinery Failure Prevention Technology, Virginia Beach, VA, USA. Application of Torsional Vibration Measurement to Shaft Crack Monitoring in Power Plants.
16. Schanze, T., 1995 IEEE Transactions on Signal Processing, 43(6). Sinc Interpolation of Discrete Periodic Signals.

List of Symbols

FFT – Fast Fourier Transform

f – frequency

Im – Imaginary part of a complex values quantity

$i = \sqrt{-1}$

k – index correspond to an integer order

min – selects the minimum of complex valued arguments on a norm basis

N – FFT block size

n – array index

o – order

O – number of angular sampling increments per shaft revolution

Re – real part of a complex valued quantity

r – array index

t – continuous time variable

t_r – discrete time array in integer multiples of Δt

$t(\theta_r)$ – time array corresponding the fixed angular sample at θ_r

$X(o_n)$ – order domain discrete Fourier transform

$\tilde{X}(o_n)$ – order domain discrete Fourier transform with integer order content removed

$\tilde{X}(f_n)$ – frequency domain discrete Fourier transform with integer order content removed

$x(t)$ – continuous function of time, or an analog signal

$x(t_r)$ – discrete array sampled with a fixed time incremental basis, Δt

$\tilde{x}(t_r)$ – discrete array sampled with a fixed time incremental basis, Δt , with integer order content removed

$x(\theta_r)$ – discrete array sampled with a fixed angular incremental basis, $\Delta\theta$

$\tilde{x}(\theta_r)$ – discrete array sampled with a fixed angular incremental basis, $\Delta\theta$, with integer order content removed

Δt – time based sampling interval

$\Delta\theta$ – angle based sampling interval

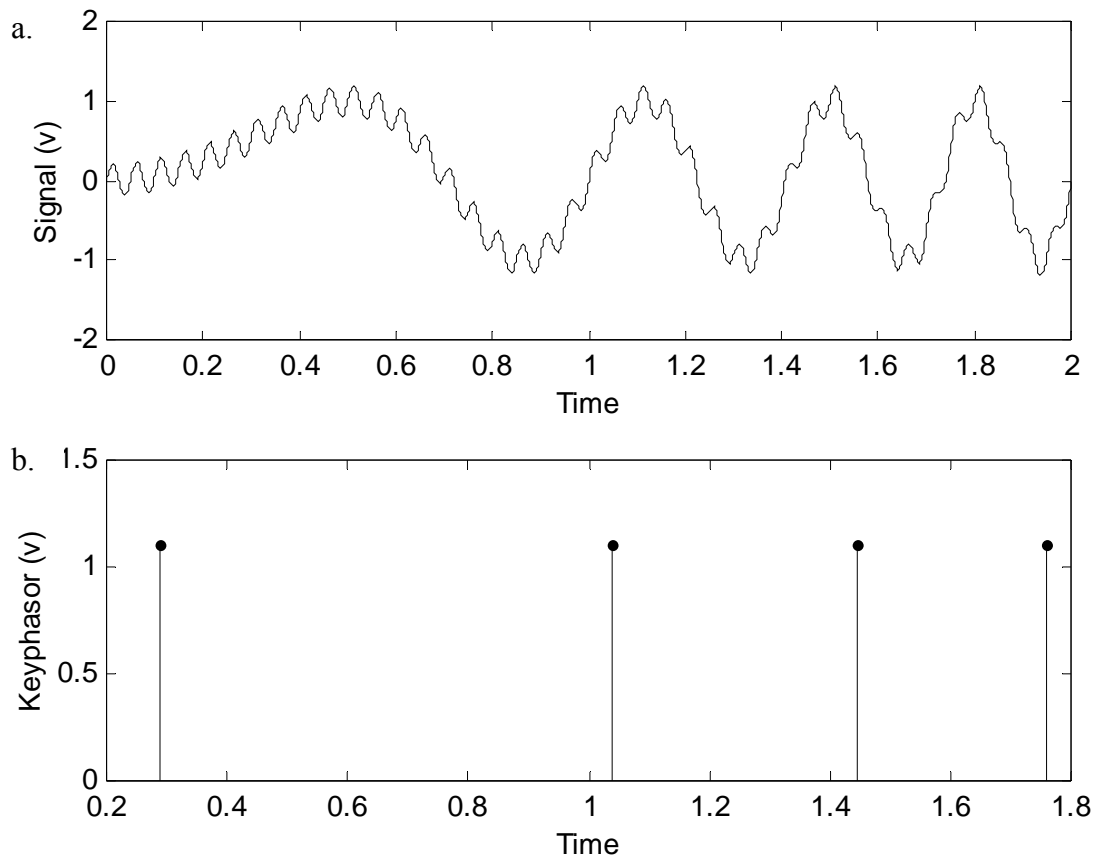


Figure 1. Signal from a simulated piece of rotating equipment.

- a. Analog dynamic signal
- b. Once per revolution keyphasor

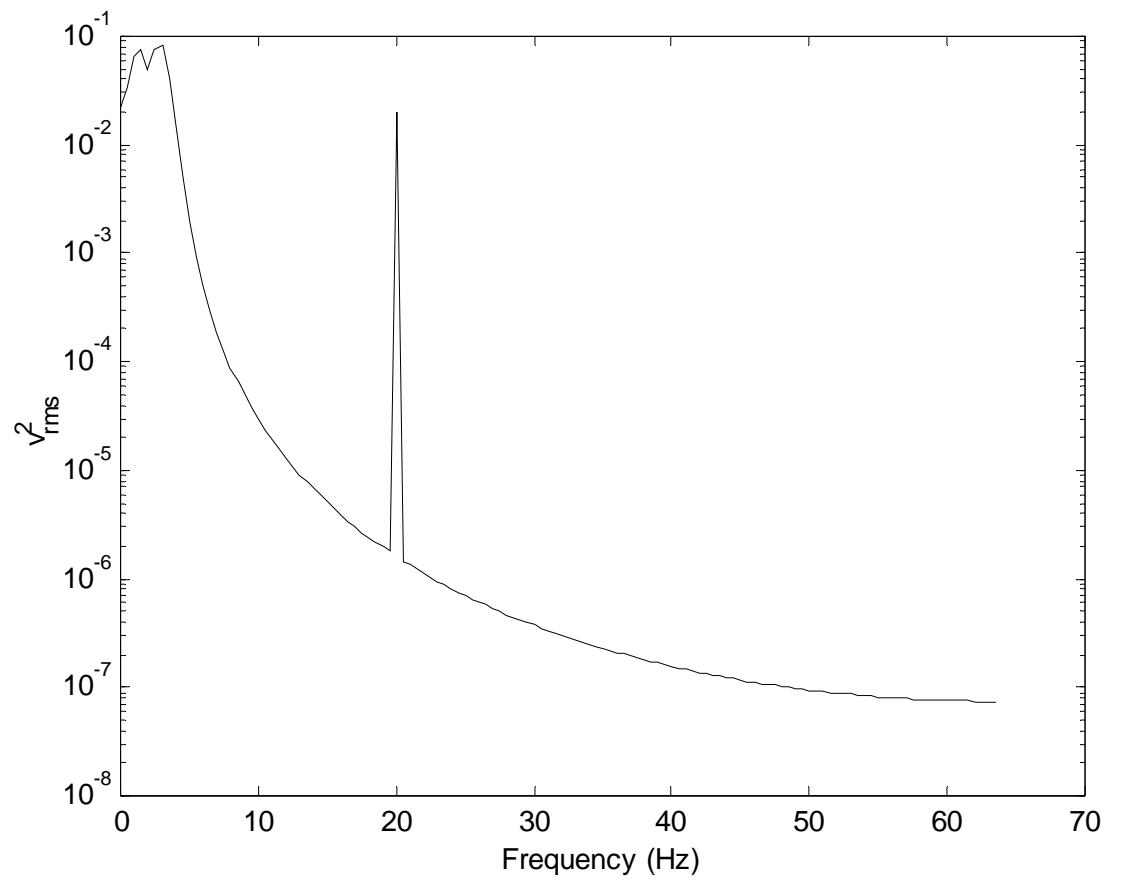


Figure 2. Spectrum of dynamic signal in Figure 1A sampled with a constant time interval (Δt).

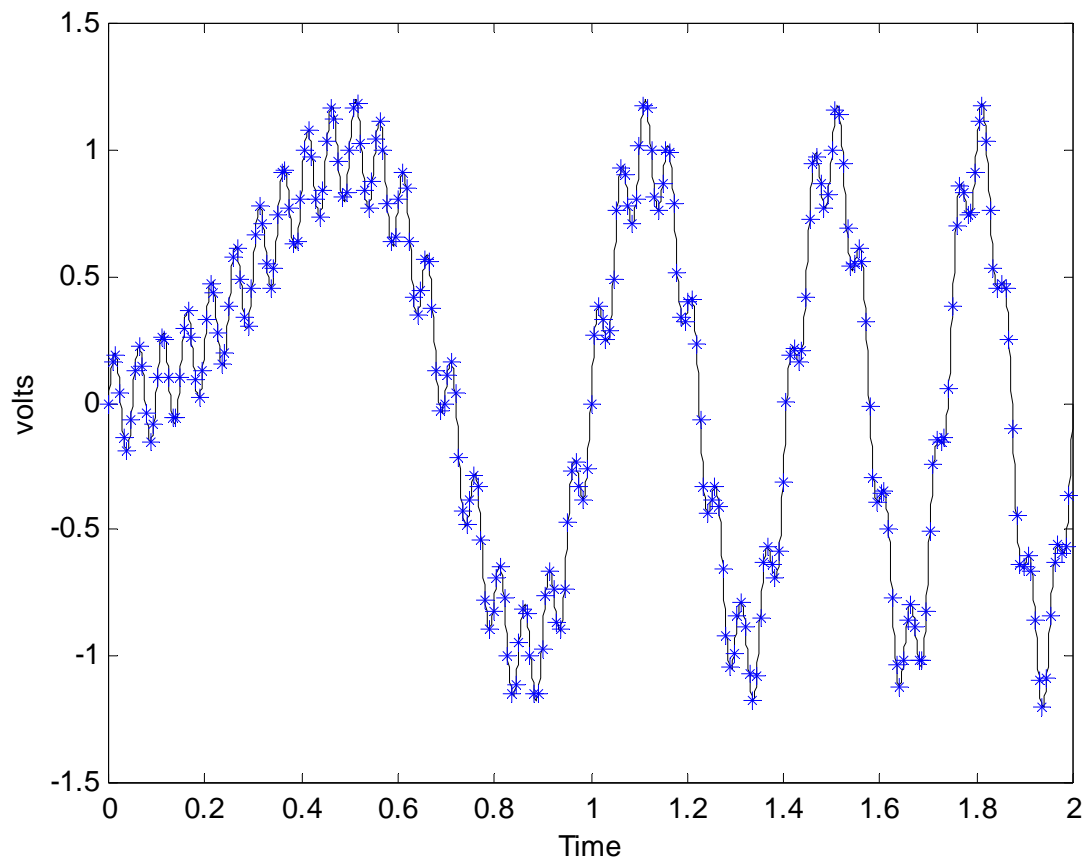


Figure 3. Analog signal from a simulated piece of rotating equipment and the corresponding discrete array sampled with a constant time interval (Δt).

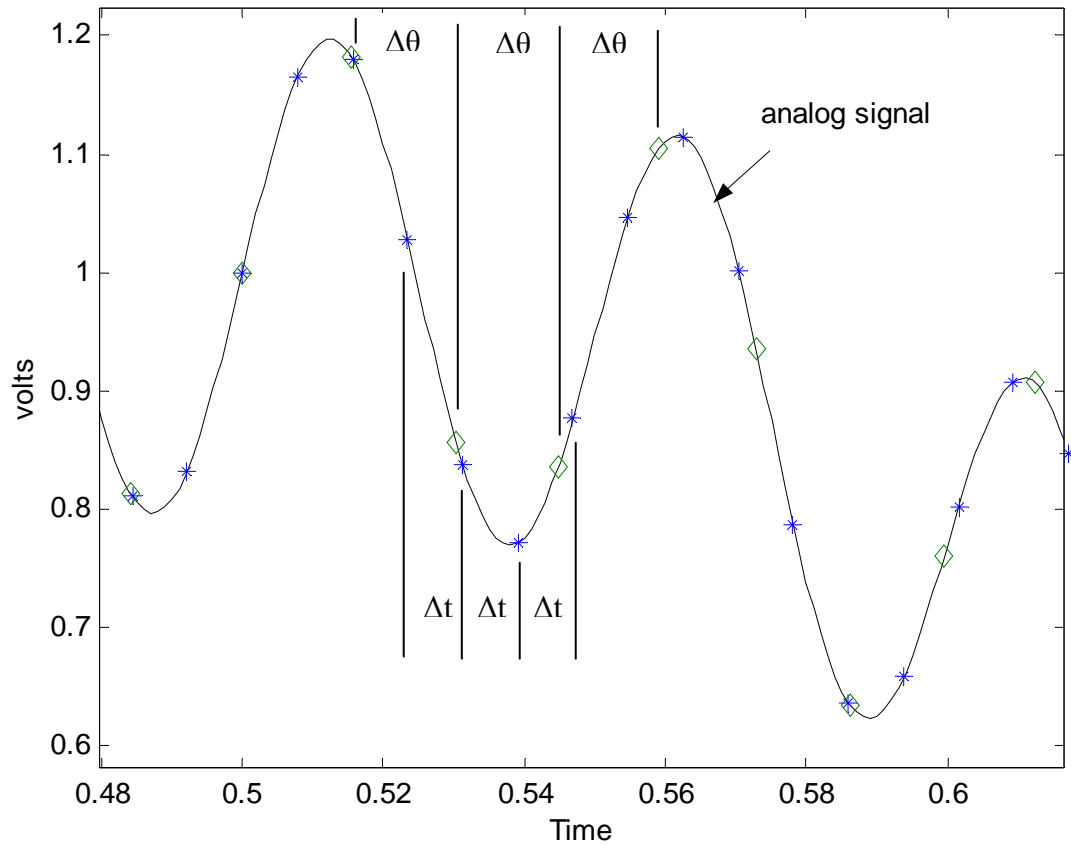


Figure 4. Analog signal from a simulated piece of rotating equipment with discrete arrays; * constant time sampling interval (Δt); \diamond constant angle sampling interval ($\Delta\theta$).

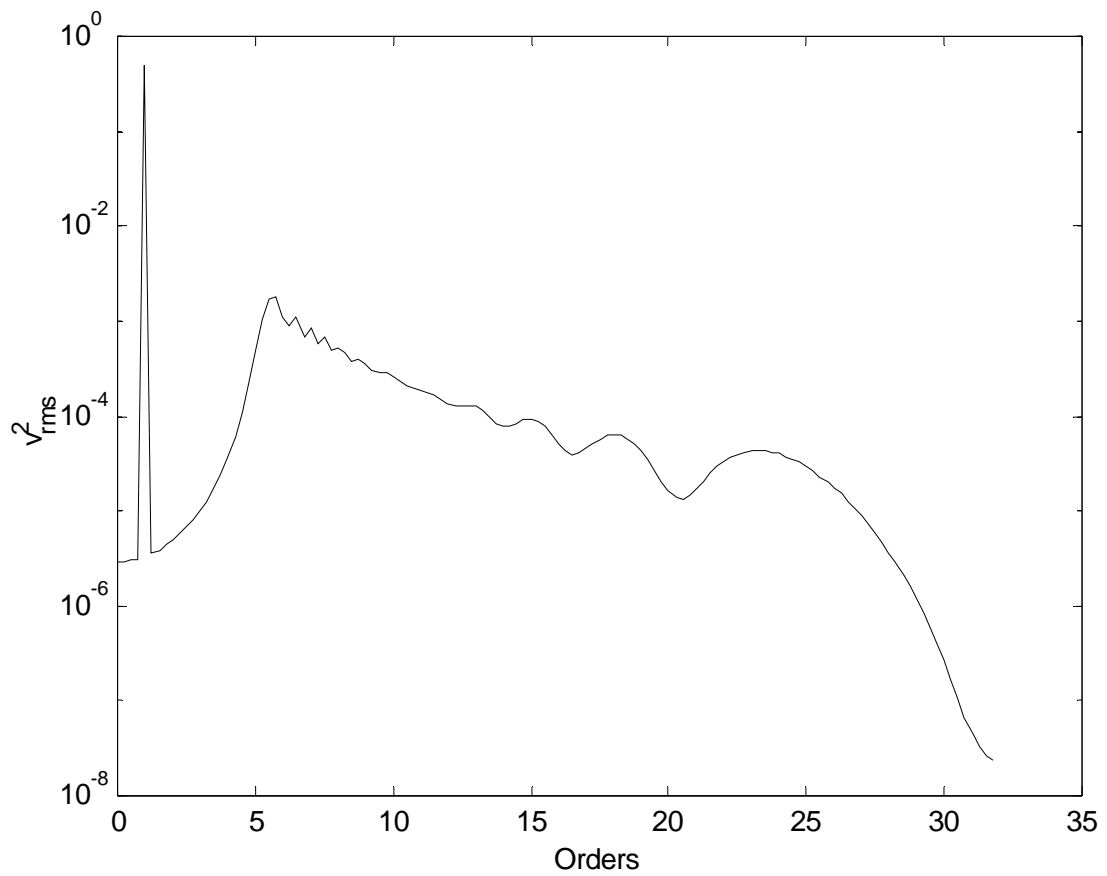


Figure 5. Order spectrum of signal from a simulated rotating equipment in Figure 1 with constant angle interval samples ($\Delta\theta$) via computed order sampling method.

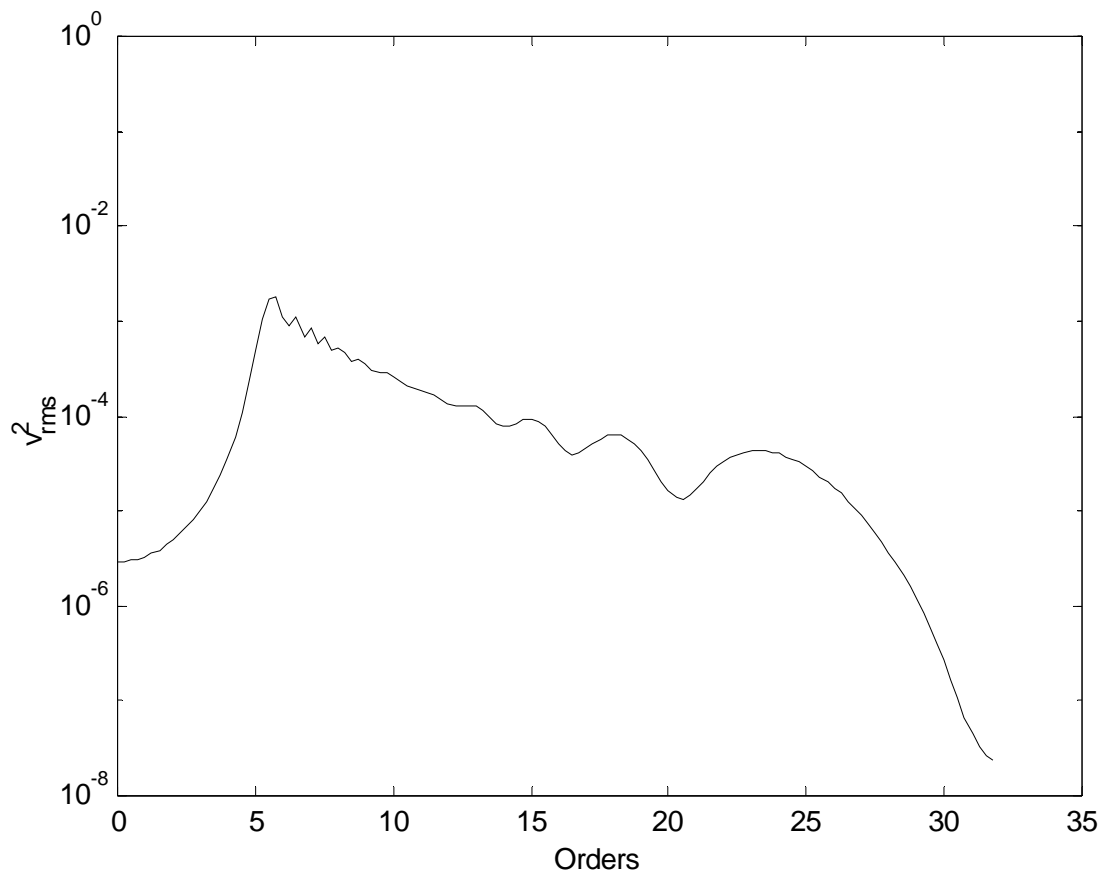


Figure 6. Order spectrum of signal from a simulated rotating equipment in Figure 1 with order content removed.

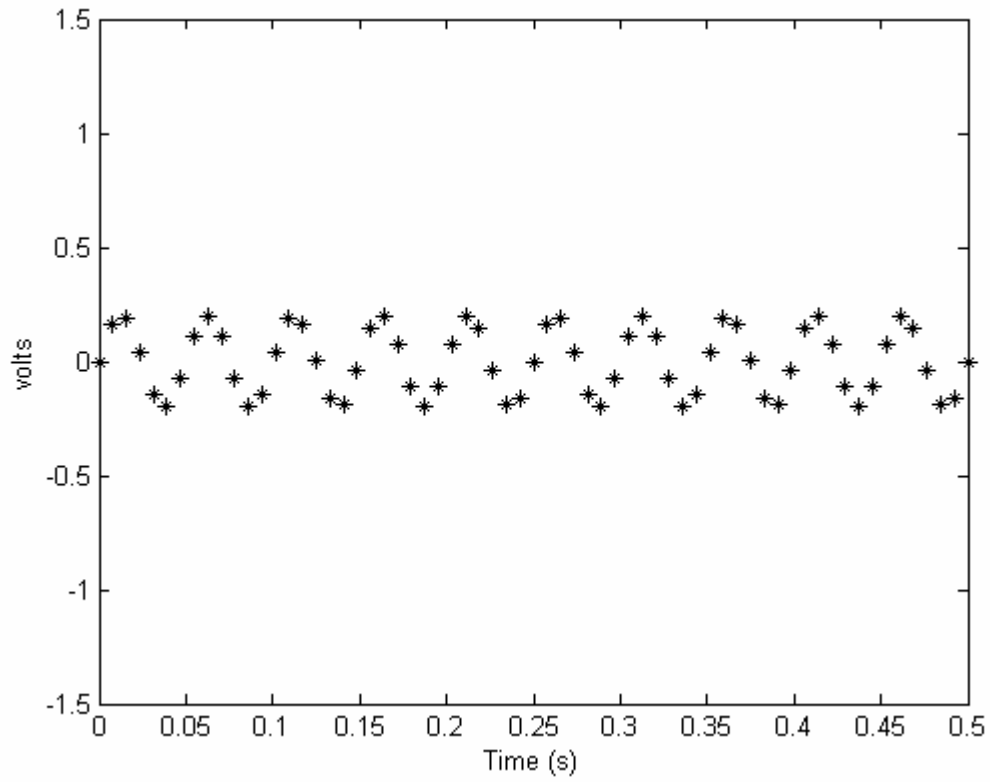


Figure 7. Double resampled time waveform in Figure 1 with order content removed.

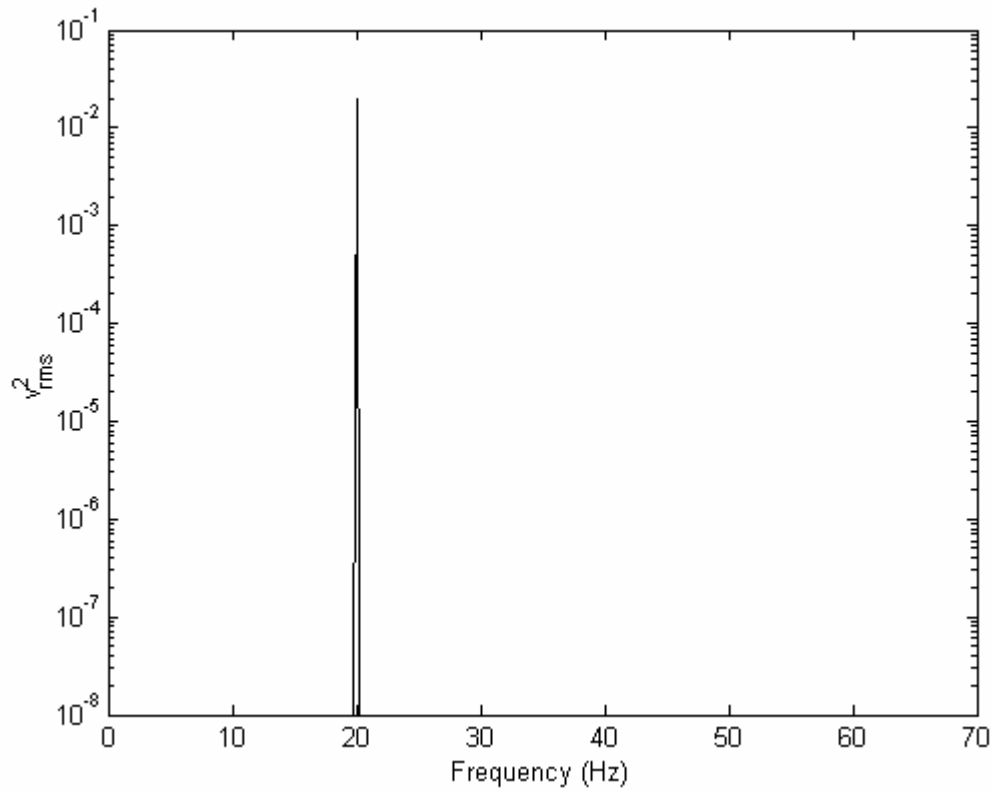


Figure 8. Double re-sampled spectrum for time waveform in Figure 1 with order content removed.

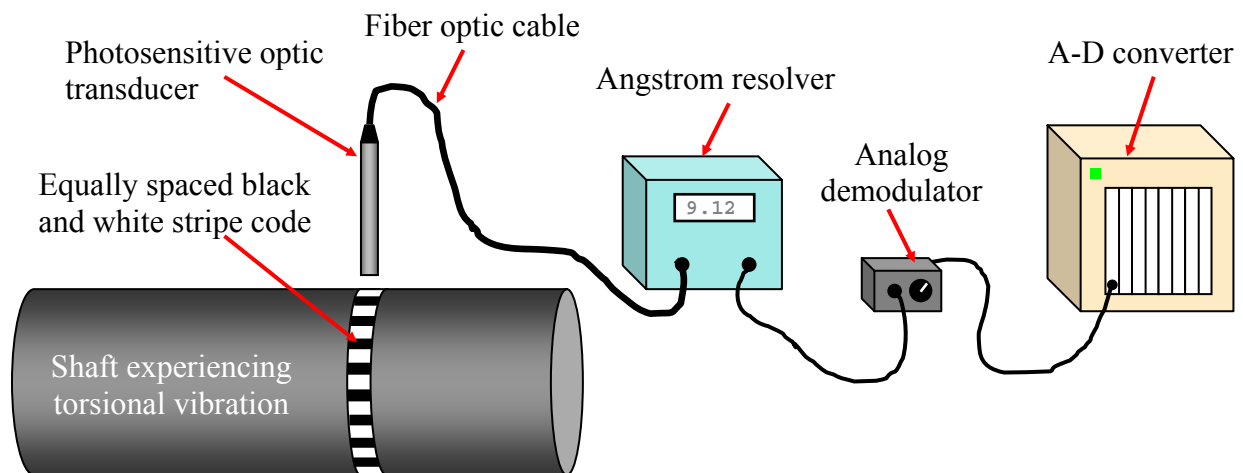


Figure 9. Schematic of torsional vibration measurement system on a rotating shaft.

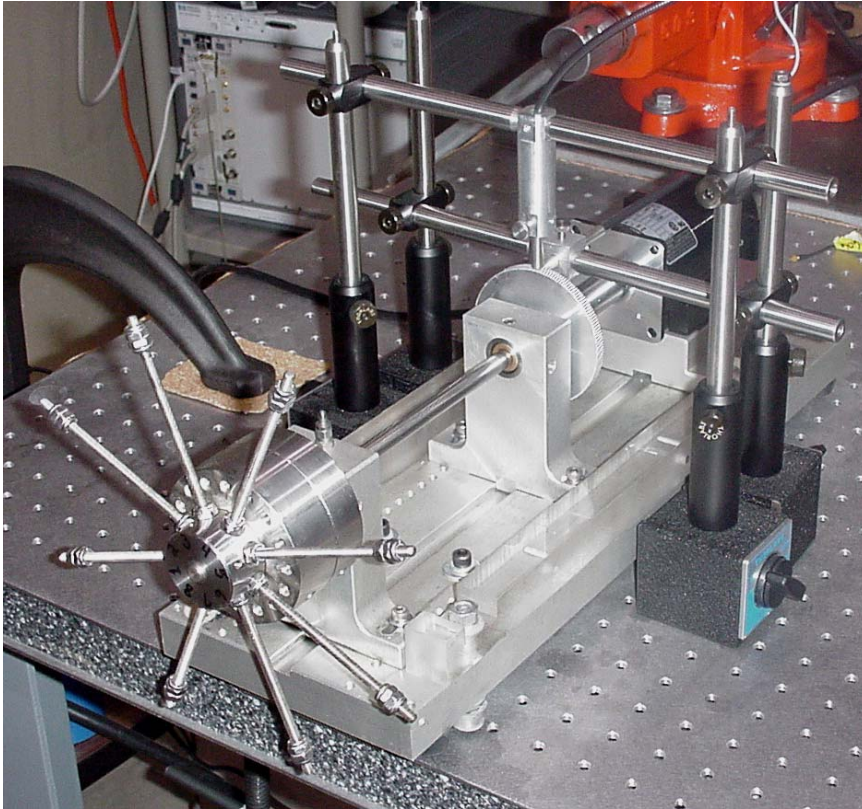


Figure 10. Torsional vibration test stand.

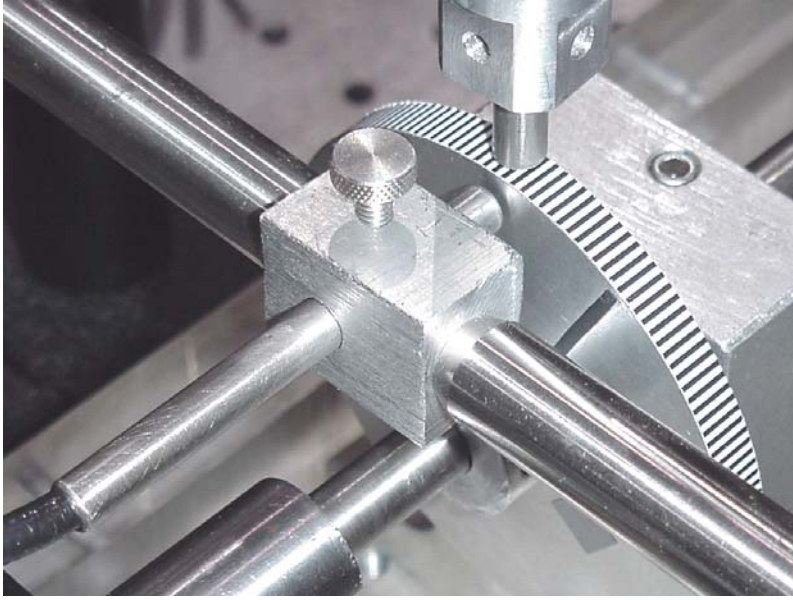


Figure 11. Close up of torsional vibration zebra tape installation and fiber optic transducer placement.

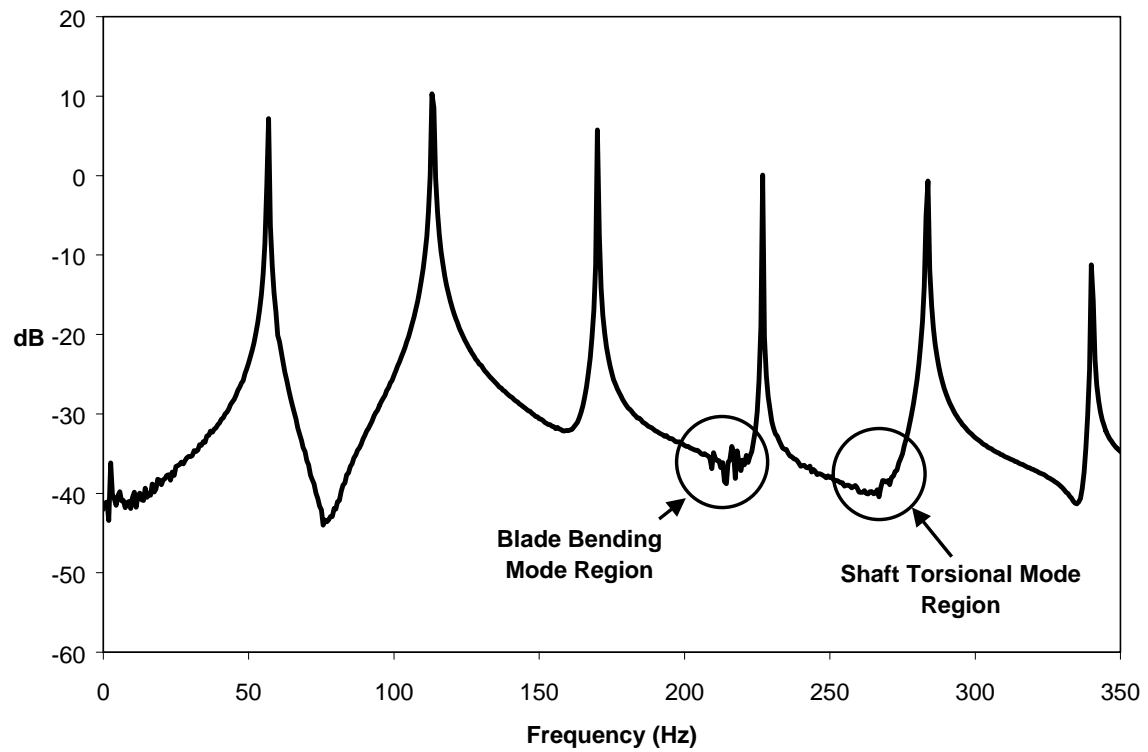


Figure 12. Torsional vibration spectrum from experimental test stand in Fig. (10) with a running speed of 3420 rpm (57 Hz), with 30 ensemble averages.

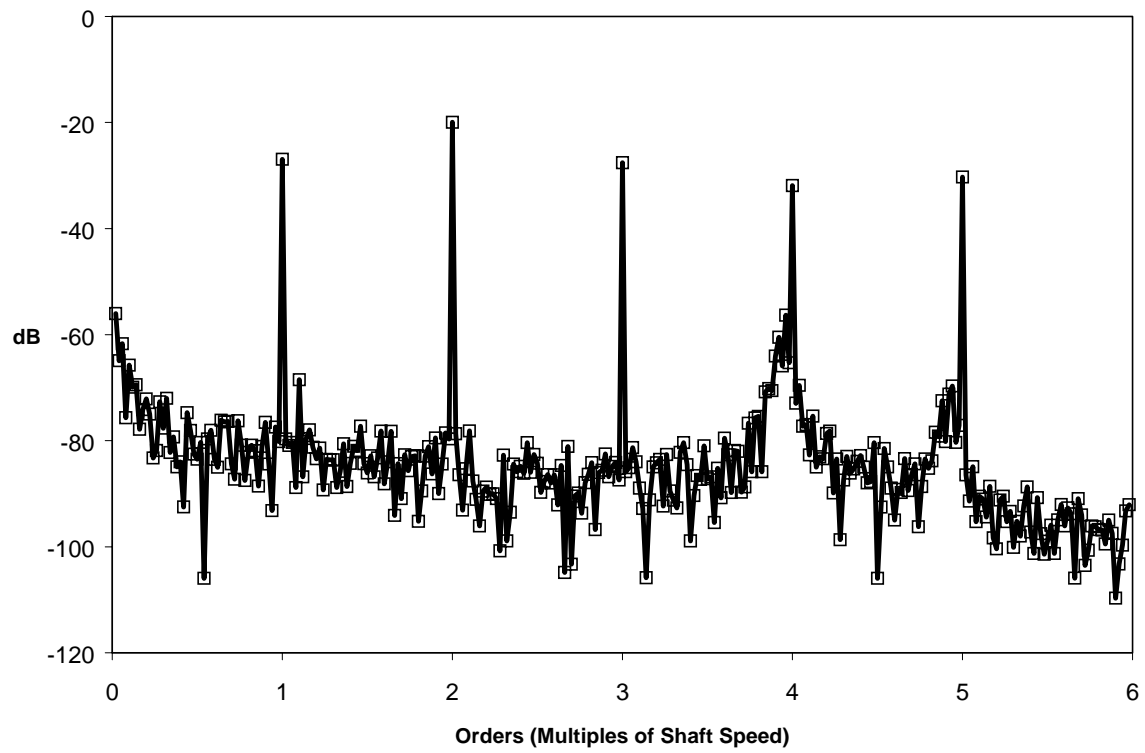


Figure 13. Order domain spectrum for a single record.

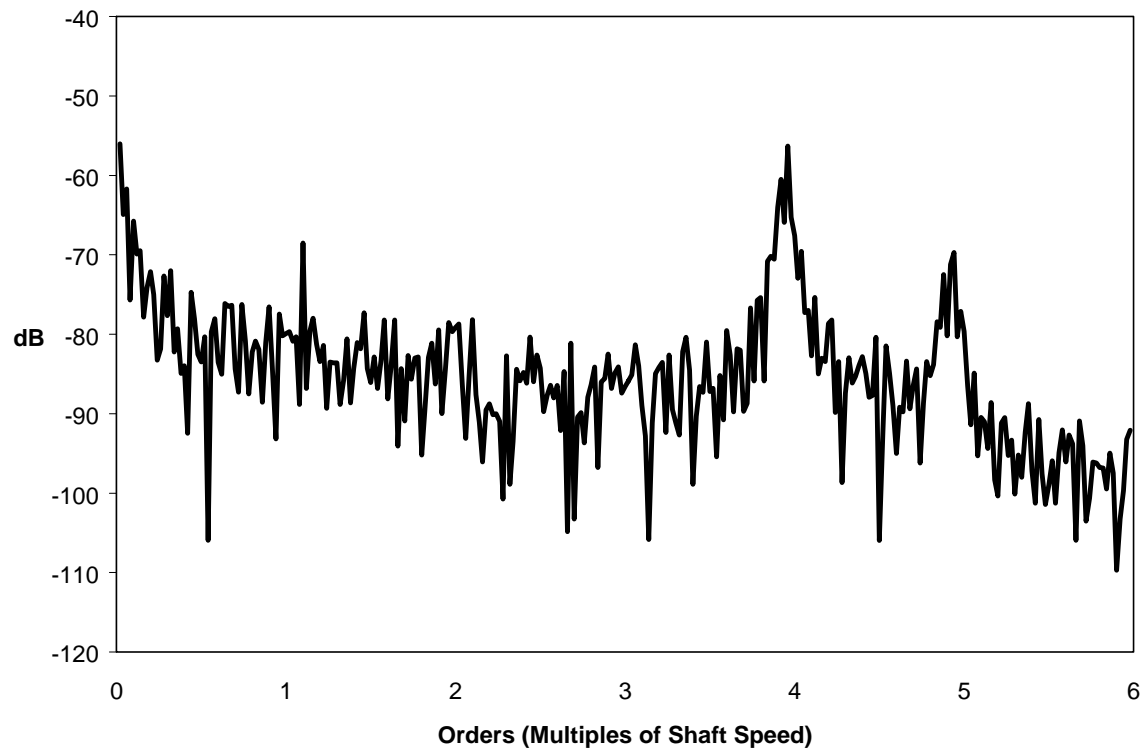


Figure 14. Order domain spectrum with order content removed for one ensemble sample.

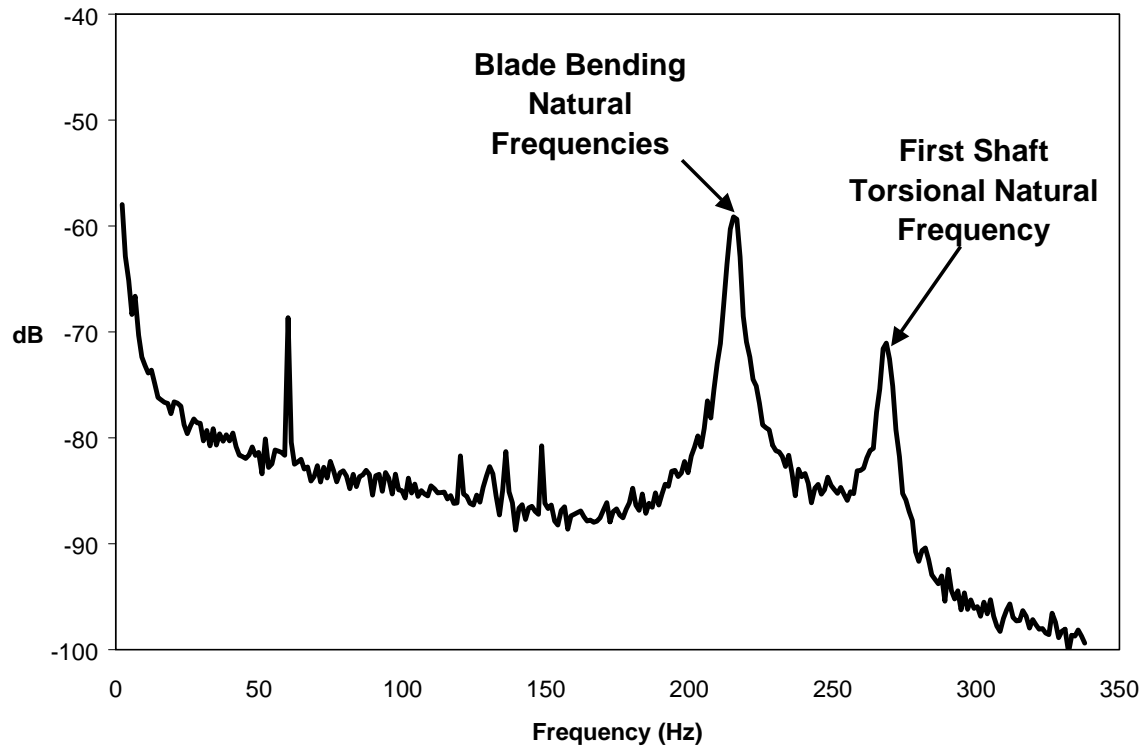


Figure 15. Torsional vibration spectrum in Fig. (12) after the order removal processing has been applied with 30 ensemble averages.